Detection of RFI by its Amplitude Probability Distribution

Christopher Ruf, Sidharth Misra, Steve Gross and Roger De Roo
The University of Michigan
Ann Arbor, MI 48109-2143

Abstract— A new type of microwave radiometer detector has been developed that is capable of identifying low level Radio Frequency Interference (RFI) and of reducing or eliminating its effect on the measured brightness temperature. The Agile Digital Detector (ADD) can discriminate between RFI and natural thermal emission signals by directly measuring higher order moments of the signal than the variance that is traditionally measured. After detection, the ADD then uses spectral and temporal filtering methods to selectively remove the RFI. ADD performance has been experimentally verified and its performance characterized while connected to an airborne C-Band radiometer (the NOAA/ETL PSR) installed on a NASA WB-57 flying over major urban centers.

***Index Terms*—microwave radiometer, radio frequency interference**

I. Introduction

The ADD consists of an analog-to-digital converter (ADC) followed by a digital signal processing (DSP) module and a data handling subsystem [1]. Analog radiometer signals enter the ADD in place of what would ordinarily be the radiometer's detection stage. The DSP module first performs digital sub band filtering and then measures the first four moments of the signal's probability density function for each sub band. The second moment reproduces the function of a standard square law detector. Algorithms that are based on higher order moments are used to detect the presence of RFI. The second moments of sub bands that are free of RFI are averaged together in post processing to produce a clean brightness temperature (T_B). Whenever RFI is a potential problem, the ADD should be considered as an alternative to the analog detector that has historically been used by microwave radiometers.

Radiometer signals are generated by noise and so are inherently random processes. In the absence of RFI, the pre-detection analog signal in a microwave radiometer is generated exclusively by thermal emission sources. These sources include both the natural thermal emission incident on the antenna from the Earth and sky as well as the radiometer noise generated by ohmic losses and noisy active components in the hardware. In this case, the PDF of the amplitude of the signal is gaussian distributed. Signal sources other than thermal noise will, in almost all cases, have non-gaussian PDFs. Leveraging this fact is the basis of the ADD approach.

II. Measurement of Kurtosis

The system noise temperature ($T_{sys} = T_B$ + receiver noise temperature) measured by a radiometer is proportional to the variance, or 2nd central moment, of its pre-detection signal, or

$$T_{sys} \propto m_2 = \left\langle (x - \langle x \rangle)^2 \right\rangle \tag{1}$$

where x(t) is the pre-detection signal and its expectation is, in practice, approximated by an average over time. The ADD measures the first four raw moments of the pre-detection signal (*i.e.* $\langle x \rangle$, $\langle x^2 \rangle$,$\langle x^3 \rangle$ and $\langle x^4 \rangle$). The 2nd central moment is derived from the measurements by

$$m_2 = \langle x^2 \rangle - \langle x \rangle^2 \tag{2}$$

Similarly, the 4th central moment is given by

$$m_4 = \left\langle (x - \langle x \rangle)^4 \right\rangle \tag{3}$$

and m_4 is derived from the measurements by

$$m_4 = \langle x^4 \rangle - 4\langle x^3 \rangle\langle x \rangle + 6\langle x^2 \rangle\langle x \rangle^2 - 3\langle x \rangle^4 \tag{4}$$

The kurtosis of the pre-detection signal, defined as the ratio between the 4th and the square of the 2nd central moments, can be derived from the measurements by

$$k = m_4/(m_2)^2 \tag{5}$$

For a gaussian distributed signal, the kurtosis is always equal to 3, independent of its variance. Thus, so long as a radiometer is observing natural thermal emission, the kurtosis will be 3, independent of variations in the brightness temperature. In case the signal is corrupted by RFI, the amplitude probability may deviate from a gaussian distribution and the value of the kurtosis may deviate from 3.

III. Kurtosis in the Presence of Pulsed Sinusoidal RFI

The behavior of the kurtosis can be characterized when observing thermal emission in the presence of a radar-like source of RFI. Assume that the RFI can be modeled as a

pulsed sinusoid with a duty cycle d and amplitude A. The probability distribution functions for the thermal emission and RFI signals are respectively represented by g(x) and f(x)

$$g(x) = \frac{1}{\sigma\sqrt{2\pi}} e^{\frac{-x^2}{2\sigma^2}} \tag{6}$$

$$f(x) = (1-d)\delta(x) + \frac{d}{\pi\sqrt{A^2 - x^2}} \tag{7}$$

Because the two signals can be considered statistically independent, the probability distribution of the composite signal is given by a normalized version of the convolution of the above two equations, or

$$r(x) = f(x) * g(x) \tag{8}$$

In order to calculate the kurtosis, we require the first four moments of the resultant signal. Derivation of the moments of the resultant signal is aided by expansion in terms of the moments of the individual signals, according to

$$m_1^{g+f} = m_1^g + m_1^f \tag{9a}$$

$$m_2^{g+f} = m_2^g + 2m_1^g m_1^f + m_2^f \tag{9b}$$

$$m_3^{g+f} = m_3^g + 3m_1^g m_2^f + 3m_2^g m_1^f + m_3^f \tag{9c}$$

$$\begin{aligned} m_4^{g+f} &= m_4^g + 4m_1^g m_3^f + 4m_2^g m_2^f + 2m_2^g m_1^f m_1^f \\ &+ 2m_1^g m_1^g m_2^f - 2m_1^g m_1^f m_1^g m_1^f + 4m_3^g m_1^f + m_4^f \end{aligned} \tag{9d}$$

Thus, the first four moments for the resultant signal become

$$m_1^{g+f} = 0 \tag{10a}$$

$$m_2^{g+f} = \sigma^2 + \frac{dA^2}{2} \tag{10b}$$

$$m_3^{g+f} = 0 \tag{10c}$$

$$m_4^{g+f} = 3\sigma^4 + 2nA^2\sigma^2 + \frac{3nA^4}{8} \tag{10d}$$

The kurtosis for a gaussian distributed signal is given by

$$R = \frac{m_4}{m_2^2} = \frac{3\sigma^4}{(\sigma^2)^2} = 3 \tag{11}$$

In the presence of pulsed-sinusoidal RFI, the moment ratio becomes

$$R = \frac{m_4^{g+f}}{(m_2^{g+f})^2} = \frac{3\sigma^4 + 2dA^2\sigma^2 + \frac{3dA^4}{8}}{\left(\sigma^2 + \frac{dA^2}{2}\right)^2} \tag{12}$$

IV. Kurtosis and Pulsed Sinusoid Duty Cycle

Numerical simulations were performed to examine the response of the kurtosis to pulsed and continuous sinusoidal RFI. Radiometric noise was generated by a gaussian random number generator. A sinusoidal signal was added to the noise. The sinusoid was gated by 2 μs pulses. The duty cycle of the pulses and the amplitude of the sinusoid were varied parametrically to evaluate their effect on the moment ratio. The results are shown in Figure 1. The y-axis in the figure is the normalized kurtosis (k/3). The x-axis, labeled SNR, is the ratio between the variance of the sinusoid and that of the gaussian noise signal. This corresponds to the relative T_B of the two signals.

In curve (a) of Figure 1, the duty cycle of the sinusoid is fixed at 1% and its amplitude is varied. The normalized moment ratio begins to rise above one as the SNR increases above -40 dB. For high values of the SNR, the moment ratio saturates at a value of approximately 3.4. The saturation is caused by the 7-bit digitizer, which "pins" at signal amplitudes of -63 and +64.

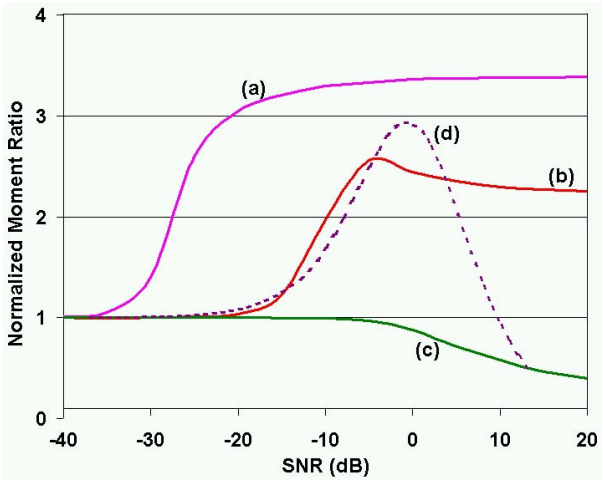

Figure 1. Numerical simulation of the dependence of the Normalized kurtosis on the strength of pulsed (2 μs pulse width) sinusoidal RFI with 1% (a), 10% (b) and 100% (c) duty cycle and variable amplitude; or (d) fixed amplitude and variable duty cycle.

Curve (b) of Figure 1 assumes a fixed duty cycle of 10% for the pulsed sinusoid while its amplitude is varied to affect the SNR. The effect of the signal on the moment ratio does not become noticeable until the SNR exceeds –25 dB. This decrease in sensitivity to RFI, relative to a 1% duty cycle, results because, with the higher duty cycle, a smaller amplitude sinusoid is required to produce a given SNR.

Curve (c) of Figure 1 assumes a duty cycle of 100% for the sinusoid (*i.e.* a continuous signal). The normalized moment

ratio for a sinusoid alone is exactly one-half. In the figure, the ratio can be seen to drop monotonically from one toward one-half as the amplitude of the sinusoid increases. At very high amplitudes, it decreases below one-half due to distortion resulting from saturation of the 7-bit digitizer. The fact that the moment ratio increases for low values of the duty cycle but decreases with a duty cycle of 100% implies that there is some intermediate duty cycle for which the moment ratio will be unchanged and, hence, insensitive to RFI. This condition is assessed in curve (d) of Figure 1, which plots the moment ratio assuming a constant amplitude sinusoid but variable duty cycle. At very low values of SNR (and of duty cycle), the moment ratio increases above one. The ratio reaches a peak of 2.9 at an SNR slightly below 0 dB (duty cycle = 4%) and then begins to decrease. The ratio passes through one at an SNR of 10 dB (duty cycle of 50%) and then decreases further. Thus, there is a "blind spot" in detection of the pulsed sinusoidal signal if the duty cycle is 50%.

V. AIRBORNE DEMONSTRATION

Results of the ADD performance during an airborne field trial was performed in August 2005 with the ADD installed in parallel with the standard back-end detector subsystem of the stepped-LO C-Band channel of the NOAA/ETL Polarimetric Scanning Radiometer (PSR). The ADD was operated during one ~2 hour flight that began and ended near Houston, TX and included overflights of the Dallas-Fort Worth and San Antonio urban areas, more rural portions of east-central Texas, and a brief period out over the Gulf of Mexico. A 60 second sample of the raw measurements while over Dallas is included here, to illustrate ADD performance in the presence of RFI. Time/frequency plots of the kurtosis and of the 2nd moment of the measurements are shown in Figures 2 and 3, respectively. In Figure 2, RFI-free regions are distinguishable by a normalized kurtosis value (kurtosis/3) of unity. There are two broad regions of the time/frequency space that are free of RFI. They cover frequency channels 171-176 (roughly 7.45-7.50 GHz) during elapsed times 0-25 and 40-50 seconds. Elsewhere, strong excursions of the kurtosis from unity are evident. In figure 3, some of the time/frequency regions with RFI also clearly show spikes of high 2nd moment. RFI in these instances could likely be identified by conventional RFI detection algorithms based solely on the 2nd moment. However, as one counterexample, consider the variations in the 2nd moment at frequency channel 170. The RFI-free elapsed times 0-25 seconds are not noticeably distinguishable from the variations during times 25-40 seconds, when the kurtosis clearly indicates the presence of RFI. A conventional RFI detection algorithm would have considerably more difficulty with this sequence of measurements.

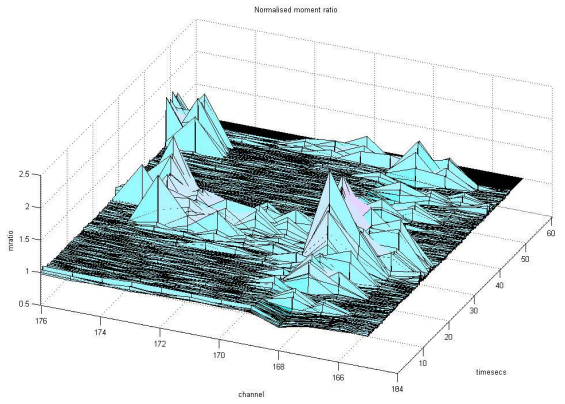

Figure 2. Normalized kurtosis while flying over Dallas. Channel numbers 176-184 roughly correspond to frequencies between 7.4 and 7.5 GHz. The time axis is elapsed time over one minute of data taking.

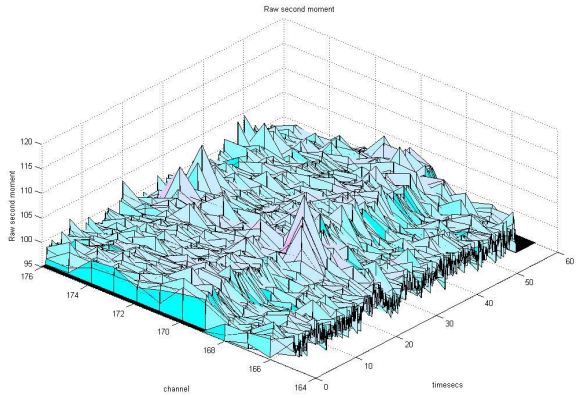

Figure 3. Second moment of measurements during the same period of time as shown in Figure 2. The 2nd moment is linearly proportional to the detected system noise temperature. Spikes in the 2nd moment tend to be associated with the presence of RFI.

ACKNOWLEDGMENTS

The authors would like to acknowledge their collaboration with the NOAA/ETL PSR team, and in particular the assistance of Dr. Albin Gasiewski. Support for the ADD team was provided by the NASA Earth Science Technology Office under grants NNG05GB08G and NNG05GL97G.

REFERENCES

[1] Ruf, C., S.M. Gross, S. Misra, "RFI detection and mitigation for microwave radiometry with an agile digital detector," IEEE Trans. Geosci. Remote Sens., **44**(3), 2006.